An Intelligent Contraflow Control Method for Real-Time Optimal Traffic Scheduling Using Artificial Neural Network, Fuzzy Pattern Recognition, and Optimization

D. Xue and Z. Dong

***Abstract*—Contraflow operation is frequently used for reducing traffic congestion near tunnels and bridges where traffic demands from the opposite directions vary periodically. In this work, a generic real-time optimal contraflow control method has been introduced. The introduced method integrates two important functional components: 1) an intelligent system with artificial neural network and fuzzy pattern recognition to accurately estimate the current traffic demands and predict the coming traffic demands, and 2) a mixed-variable, multilevel, constrained optimization to identify the optimal control parameters. Application of the developed method to a case study—dynamic contraflow traffic operation at the George Massey Tunnel in Vancouver, BC, Canada has significantly reduced traffic delay and congestion.**

***Index Terms*—Fuzzy pattern recognition, neural network, optimization, real time systems, traffic control.**

I. Introduction

A. Background

TUNNELS and bridges are often bottlenecks of a traffic system and sources of traffic congestion. The time-varying unbalanced traffic flow during rush hours frequently imposes heavy traffic demand on one side of the road, while showing light traffic demand on the opposite side. A contraflow operation, which periodically switches one or more traffic lanes from one direction to the opposite direction, is often employed to reduce congestion on the busy side.

Most of the presently used control methods for a contraflow operation are static in nature. These approaches operate on a few fixed contraflow control schedules that were generated based upon the statistical traffic demands over certain time periods. The mismatch between a fixed contraflow control schedule and the dynamic varying traffic demand often leads to poor system performance. A dynamic contraflow operation control method, that generates the optimal control parameters based on the real-time data, is in great need. This work focuses on the development of such a new method.

A. Related Work

Presently many urban traffic control (UTC) systems are used to reduce traffic delay caused by congestion through the effective control and coordination of traffic signals in urban traffic networks [1], [2]. Most of these UTC systems were developed based upon static traffic control approach using fixed timing plans to coordinate traffic signals. With recent advances in real-time control, instrumentation, and computer networks, various dynamic control methods, that continuously adjust traffic signal timing plans using the collected real-time traffic flow data, were introduced to UTC systems [1]. Typical adaptive UTC systems include the SCOOT system in the United Kingdom [3], the SCATS system in Australia [4], and a number of others [1]. In addition, many advanced soft computing techniques, including neural networks, fuzzy logic, and optimization, have been used in developing dynamic traffic control systems as part of the Intelligent Transportation Systems (ITS) [5].

However, most of the present traffic control systems are developed with very low accuracy. For instance, the traffic flow estimation errors caused by traffic congestion are seldom studied and compensated. Most of these systems update their timing plans only after a significant change in traffic flow is identified. The lack of the capability of accurately estimating current traffic demand and predicting future traffic demand leads to a constant lag in the traffic control.

B. George Massey Tunnel Contraflow Control Problem

The George Massey Tunnel is a traffic bottleneck between two suburban cities—Richmond and Delta in the greater Vancouver area. Four lanes are in the tunnel, two for northbound traffic and two for southbound traffic. Since more vehicles travel in northbound toward the city center during morning traffic peak hours, three lanes are open to the northbound traffic and one lane to the southbound traffic. During the afternoon traffic peak hours, on the other hand, three lanes are opened in the southbound direction and one in the northbound direction, to accommodate the large leaving-city traffic demand. Each contraflow operation cycle consists of four steps: 1) closing the selected contraflow lane to clear up traffic on the lane; 2) opening the contraflow lane in the opposite direction; 3) closing the contraflow lane when the traffic peak hours are over; and 4) reopening the traffic lane to its normal state.

Previously, the contraflow traffic control operated on a fixed schedule: one shift in the morning and another in the afternoon during traffic peak hours with fixed starting time and duration. To improve this static traffic control method, the Ministry of Transportation and Highways of British Columbia launched the *optimal responsive contraflow control* project in 1992. During its development, a model for estimating the traffic demand at the tunnel site using traffic flow information

Manuscript received December 15, 1997; revised October 1, 1998. Recommended by Associate Editor, N. Sundararajan. This work was supported by the British Columbia Ministry of Transportation and Highways.

D. Xue is with the Department of Mechanical and Manufacturing Engineering, The University of Calgary, Calgary, Alberta, Canada T2N 1N4 (e-mail: xue@enme.ucalgary.ca).

Z. Dong is with the Department of Mechanical Engineering, University of Victoria, Victoria, British Columbia, Canada V8W 3P6 (e-mail: zdong@me.uvic.ca).

Publisher Item Identifier S 1063-6536(00)00527-3.

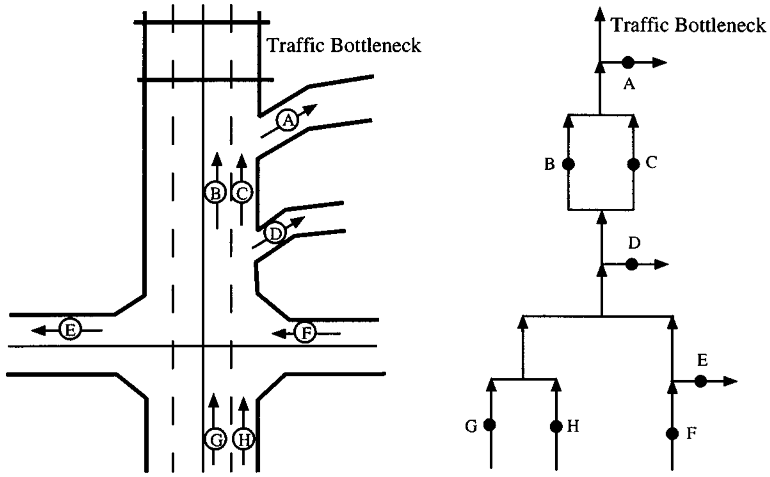

(a) Physical Traffic Network (b) Graph of Traffic Network

Layer1: D1 = B + C - A
Layer2: D2 = G + H + F - E - D - A

D1, D2: Estimated Traffic Demands at the Bottleneck
A, B, C, D, E, F, G, H: Collected Traffic Flow Data

Fig. 1. A graph-based traffic demand estimation model.

near the tunnel was proposed [6]. Eleven traffic counters were then installed on the major roads near the tunnel to acquire traffic flow data. Calculation of traffic congestion at the tunnel site and identification of the optimal contraflow control schedule through an off-line analysis, considering one or two contraflow operation cycles, using an exhaustive search method were studied [7]. A method for predicting traffic demands by identifying the most similar historical traffic demand data set was also proposed [7]. Further study on on-line traffic demand estimation and analysis of collected traffic flow data were subsequently conducted [8], [9]. Implementation of a real-time contraflow control system was also initiated [10], [11].

However, a number of problems arose during the project. These can be summarized into three categories:

1) The model for estimating true current traffic demand at the sensing time using the on-line acquired traffic flow data was not accurate enough. The error on traffic demand estimation at the tunnel site, including the errors caused by congestion and insufficient traffic counters, were not well studied and compensated.
2) The method for predicting coming traffic demands using on-line acquired traffic data was too primitive. Historical traffic demands were regarded as "patterns" in an *ad hoc* manner. Identification of the best-fit "pattern" was carried out by matching the collected traffic data with all of pre-stored "patterns," leading to a time consuming process.
3) The method used for identifying the optimal contraflow control schedule was not efficient and accurate. The contraflow schedule optimization was simply carried out using an exhaustive search. The approach requires a relatively long computation time within the limited on-line control time frame, and leaves no time for a detailed search to achieve an accurate result.

These problems precluded the system from being used as a practical, optimal contraflow traffic control tool. The work presented in this paper addresses these technical issues and provides a new generic approach to real-time optimal contraflow control. Further technical details on this work can be found in [12]. Continuous improvement and implementation of a better user interface were also carried out at the Ministry of Transportation and Highways of British Columbia since the completion of this work.

II. Estimation of Current Traffic Demand Using Feedforward Neural Network

A. A Multilayer Dynamic Traffic Demand Estimation Model

Traffic demand at a bottleneck point of the road network, such as a tunnel or bridge, is normally estimated using the traffic flow data acquired from the roads close to the troubled spot. First a graph is derived from the physical traffic network [6], as shown in Fig. 1. From this graph, it is apparent that the traffic demand at the bottleneck can be calculated as $D1$ or $D2$.

Two types of errors are found in traffic demand estimation: 1) the errors caused by traffic congestion, and 2) the errors caused by the lack of sufficient traffic counters. For instance, during peak traffic hours, congestion may emerge near the bottleneck site, such as locations B and C in Fig. 1. The estimated traffic demand, $D1$, calculated using the traffic data acquired from these counters, is lower than the actual traffic demand. The true traffic demand can be better estimated by $D2$ using the counters further away from the bottleneck site. However, the estimated traffic demand, $D2$, is less accurate considering the time delay and lack of sufficient traffic counters at all merging and exit roads. For instance, if no counter is installed at location D (an exit road) in Fig. 1 due to its low traffic volume and less significance, the estimated traffic demand, $D2$, would be higher than the actual traffic passing through the bottleneck, i.e., some artificial traffic

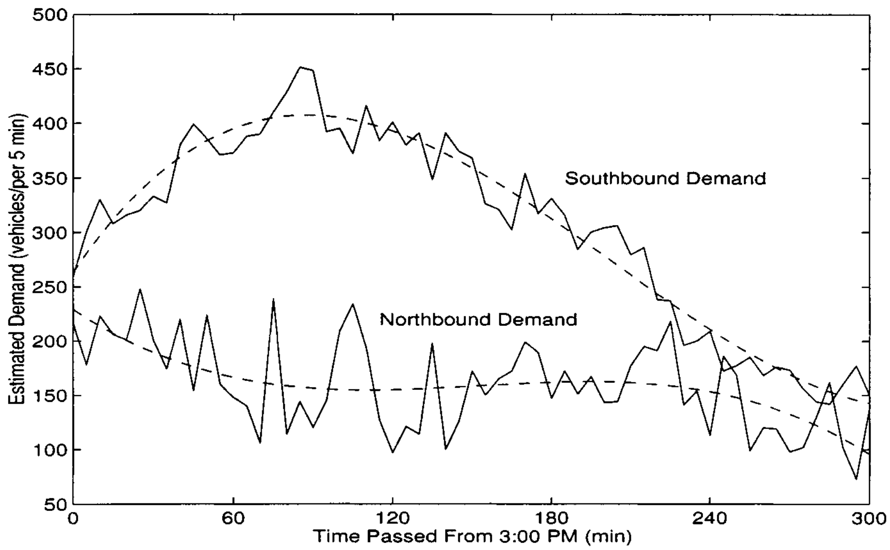

Fig. 2. Traffic demands in southbound and northbound directions.

is "added" in the traffic estimation model. Similarly, for a minor merging road some traffic might be "lost" in the traffic estimation model. More frequently, these problems are caused by malfunctioning traffic sensors or communication hardware.

A multilayer dynamic traffic demand estimation model is introduced to reduce the traffic estimation errors caused by congestion. In this model, all counters are organized in different layers based upon their distances to the bottleneck site. The layer with the traffic counters that are closer to the traffic bottleneck has higher priority for traffic demand estimation. A congestion is detected when the traffic demand calculated using the counters at one layer is significantly lower than the traffic demand calculated using the counters at a further away layer. The traffic demand will then be estimated using the next layer traffic counters. To handle the second type of traffic estimation errors, the simple vehicle number counting mechanism is replaced by an artificial neural network that is trained using real traffic flow data to remember the true behavior of the traffic system. The method will be discussed in details in the following sections.

B. Removal of Random Traffic Noise Through Least Square Curve-Fitting

Fig. 2 shows the estimated northbound and southbound traffic demand data in the afternoon at the George Massey Tunnel site. These data present the trend of traffic flow change and random noises introduced by uncontrollable factors. These random noises have to be removed due to the following reasons: 1) the random noise hinders the interpretation of the real traffic demand, 2) noise free traffic flow volumes serve as better training and operation data for the artificial neural network that is used to estimate traffic demand with incomplete data caused by missing or malfunctioning traffic counters, and 3) both computation efficiency and reliability can be improved in the process of contraflow schedule optimization using a smooth traffic demand curve without many meaningless local minima caused by random noise.

In this work, a least-square curve-fitting method is used to eliminate the high frequency noise. Suppose, $D_1, D_2, \cdots, D_m$ are m obtained traffic demand data points at time $t_1, t_2, \cdots, t_m$, and the nth polynomial curve is represented as

$$D(t) = c_0 + c_1 t + \cdots + c_n t^n \tag{1}$$

where $c_0, c_1, \cdots, c_n$ are n coefficients, the least-square curve-fitting scheme is used to obtain these coefficients of the nth polynomial by

$$\min \sum_{k=1}^{m} (D(t_k) - D_k)^2. \tag{2}$$

The coefficients are calculated using

$$\begin{bmatrix} c_0 \\ c_1 \\ \cdots \\ c_n \end{bmatrix} = [A]^{-1} \begin{bmatrix} y_0 \\ y_1 \\ \cdots \\ y_n \end{bmatrix} \tag{3}$$

where $[A]$ is a $n+1$ by $n+1$ matrix. The element a_{ij} at ith row and jth column in matrix $[A]$ is defined as

$$a_{ij} = \sum_{k=1}^{m} t_k^{i+j-2}, \qquad (i = 1, 2, \cdots, n+1; \quad j = 1, 2, \cdots, n+1) \tag{4}$$

and y_i is defined as

$$y_i = \sum_{k=1}^{m} D_k t_k^i \qquad (i = 0, 1, \cdots, n). \tag{5}$$

To balance the quality of the curve-fitting and the computation efficiency, a tenth polynomial is used. The mathematical models of traffic demand are illustrated by the smooth curves of the dashed lines shown in Fig. 2.

C. A Multilayer Feedforward Neural-Network-Based Traffic Demand Estimation Model

A multilayer feedforward artificial neural network, that is trained using the backpropagation algorithm, is an effective tool for modeling nonlinear relations among massive input and output data when the mathematical relations among these input and output parameters cannot be easily formulated [13]. In this work, a three-layer feedforward neural network, as shown in Fig. 3, is used for estimating traffic demand with possible missing or malfunctioning traffic counters. The neural network consists of nodes at three layers: an input layer with n input nodes, a hidden layer with p hidden nodes, and an output layer with one output node. The nodes at two adjacent layers are connected by arcs with weights u_{ij} $(i = 1, 2, \cdots, n;\ j = 1, 2, \cdots, p)$ and w_j $(j = 1, 2, \cdots, p)$. This neural network is first trained to formulate the input and output relations, and then used to estimate traffic demands for given input traffic data.

Training of the feedforward neural network is carried out through adjusting the weights of connection arcs by a backpropagation algorithm using a collection of correct input–output data sets. The traffic demand estimation neural network is trained through the following steps.

1) Normalize the sample correct data sets as input–output data sets for the neural network. Suppose, $V_i^{(k)} (i = 1, 2, \cdots, n;\ k = 1, 2, \cdots, m)$ is the sensed traffic flow of the ith traffic counter in the kth data set, this measure is transformed into an input data $I_i^{(k)}$ using

$$I_i^{(k)} = \frac{\left(V_i^{(k)} - V_i^{(\min)}\right) \cdot \left(I_i^{(\max)} - I_i^{(\min)}\right)}{V_i^{(\max)} - V_i^{(\min)}} + I_i^{(\min)}, \qquad (i = 1, 2, \cdots, n) \tag{6}$$

where

$V_i^{(\max)}$ upper bound value of the ith traffic flow data;
$V_i^{(\min)}$ lower bound value of the ith traffic flow data;
$I_i^{(\max)}$ upper bound value of the ith normalized input;
$I_i^{(\min)}$ lower bound value of the ith normalized input.

The output, $D^{(k)}$ $(k = 1, 2, \cdots, m)$, can be transformed into a normalized measure, $O^{(k)}$, using the same method. In this work, the normalized lower and upper bound values of an input node are selected as −5 and 5; and the normalized lower and upper bound values of an output node are selected as 0.05 and 0.9, respectively.

2) Assign random values in the range of [−1, 1] to all the connections u_{ij} and w_j, threshold values of all the hidden nodes Θ_j $(j = 1, 2, \cdots, p)$, and threshold value of the output node Γ.

3) For each normalized correct data set $(I_1^{(k)}, I_2^{(k)}, \cdots, I_n^{(k)}, O^{(k)})$;

a) Calculate the values of the hidden nodes using

$$H_j = f\left(\sum_{i=1}^{n} \left(I_i^{(k)} u_{ij}\right) + \Theta_j\right) \qquad (j = 1, 2, \cdots, p) \tag{7}$$

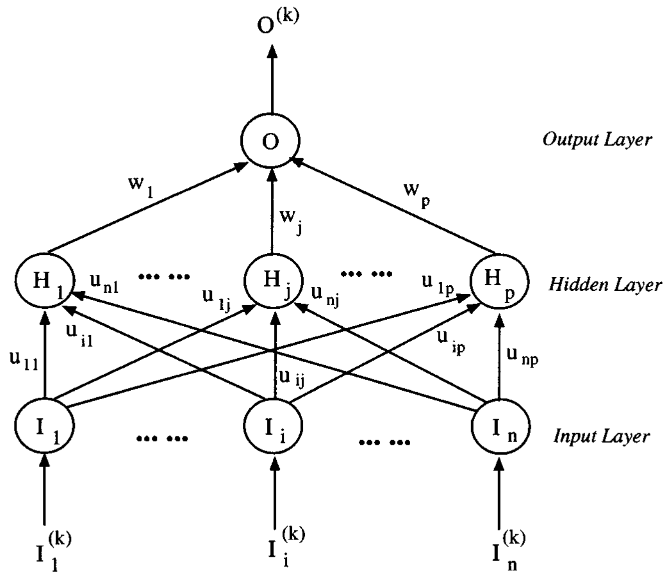

Fig. 3. A three-layer feedforward neural network for traffic demand estimation.

where $f()$ is the sigmoid function $f(x) = (1 + e^{-x})^{-1}$.

b) Calculate the value of the output node using

$$O = f\left(\sum_{j=1}^{p} (H_j w_j) + \Gamma\right). \tag{8}$$

c) Compute the error at output node using

$$d = d^{(k)} = O(1 - O)(O^{(k)} - O). \tag{9}$$

d) Compute the error of each node in the hidden node layer using

$$e_j = H_j(1 - H_j) w_j d \qquad (j = 1, 2, \cdots, p). \tag{10}$$

e) Adjust the connections from the hidden nodes to output node by

$$\Delta w_j = \alpha H_j d \qquad (j = 1, 2, \cdots, p) \tag{11}$$

where α is a learning rate selected as 1.0.

f) Adjust the connections from the input nodes to the hidden nodes by

$$\Delta u_{ij} = \beta I_i^{(k)} e_j \qquad (i = 1, 2, \cdots, n;\ j = 1, 2, \cdots, p) \tag{12}$$

where β is learning rate selected as 1.0.

4) Repeat Step 3) until the sum of errors regarding all the normalized correct data sets defined by

$$E = \tfrac{1}{2} \sum_{k=1}^{m} \left(d^{(k)}\right)^2 \tag{13}$$

is less than a specified small number ε.

In the real-time traffic demand estimation using the artificial neural network, traffic flow data collected from the major roads near the bottleneck site are first transformed into the normalized

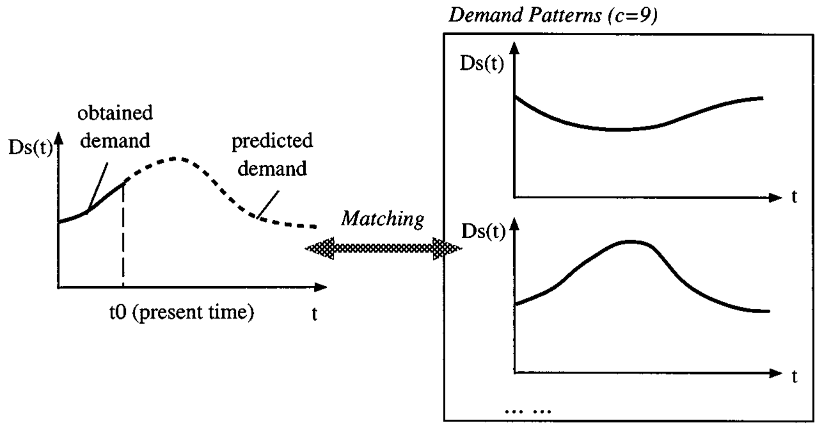

Fig. 4. Traffic demand prediction by pattern matching.

input data using (6). These normalized input data are presented to the trained neural network to calculate the normalized output using (7) and (8). The normalized output is then transformed back into traffic demand using the relation defined in (6).

III. Prediction of Coming Traffic Demands Using a Hierarchical Pattern Recognition Approach

A. A Pattern-Based Traffic Demand Prediction Model

The *present* and *past* traffic demand can be estimated directly using the collected traffic flow data. To identify the optimal contraflow control schedule, one also needs to predict the *coming* traffic demand in advance. In this research, a pattern matching approach is employed to predict the coming traffic demands, as illustrated in Fig. 4.

In this approach, historical traffic demand data during a specific time period are classified into c representative patterns. Each pattern is described by a p-dimensional vector $P_i = (P_{i1}, P_{i2}, \cdots, P_{ip})$, $(i = 1, 2, \cdots, c)$. The presently collected actual traffic demand data are represented by $D = (D_1, D_2, \cdots, D_q)$, $(q < p)$. This partial traffic demand vector is then compared with all stored traffic patterns by calculating its distances to these patterns using

$$\mathrm{distance}(D, P_i) = \sqrt{\sum_{k=1}^{q} (D_k - P_{ik})^2} \quad (i = 1, 2, \cdots, c;\, q < p). \tag{14}$$

The traffic pattern that has the minimum distance to the on-line acquired traffic demand vector over the available vector elements is identified as the best-fit traffic flow pattern P^*. The following elements of the identified best-fit traffic flow pattern are then used as the predicted coming traffic demands. The complete traffic demand vector is thus represented as

$$D' = (D_1, D_2, \cdots, D_q, P^*_{q+1}, P^*_{q+2}, \cdots, P^*_p). \tag{15}$$

B. Fuzzy Pattern Clustering

In this work, representative traffic flow patterns are identified using the fuzzy c-means clustering method [14]. In the fuzzy set theory, the relationship between an element and a set is described by a membership function in the range of [0, 1], rather than a simple "in" or "out" relation as in the classical set theory. Each of the n previously collected data sets is described by a p-dimensional vector, $D_j = (D_{j1}, D_{j2}, \cdots, D_{jp})$, $(j = 1, 2, \cdots, n)$. Suppose the number of representative traffic patterns, or cluster number, is c, a total of c traffic patterns can then be formed using the fuzzy c-means clustering algorithm through the following steps.

1) Initialize the membership μ_{ij} of D_j for cluster i $(i = 1, 2, \cdots, c)$ such that

$$\sum_{i=1}^{c} \mu_{ij} = 1. \tag{16}$$

2) Compute the fuzzy centroid vector V_i for $i = 1, 2, \cdots, c$ using

$$V_i = \frac{\sum_{j=1}^{n} (\mu_{ij})^m D_j}{\sum_{j=1}^{n} (\mu_{ij})^m} \tag{17}$$

where the fuzziness index m is a real number greater than one.

3) Update the fuzzy membership μ_{ij} by

$$\mu_{ij} = \frac{\left(\frac{1}{d^2(D_j, V_i)}\right)^{(1/(m-1))}}{\sum_{i=1}^{c} \left(\frac{1}{d^2(D_j, V_i)}\right)^{(1/(m-1))}} \tag{18}$$

where

$$d^2(D_j, V_i) = \sum_{k=1}^{p} (D_{jk} - V_{ik})^2. \tag{19}$$

4) Calculate

$$J_m = \sum_{i=1}^{c} \sum_{j=1}^{n} (\mu_{ij})^m \, d^2(D_j, V_i). \tag{20}$$

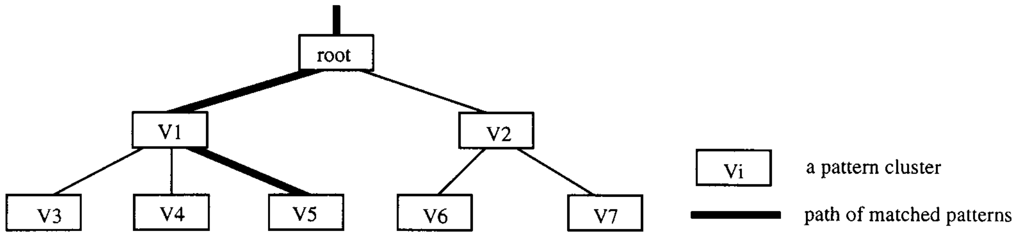

Fig. 5. Hierarchical pattern representation and matching.

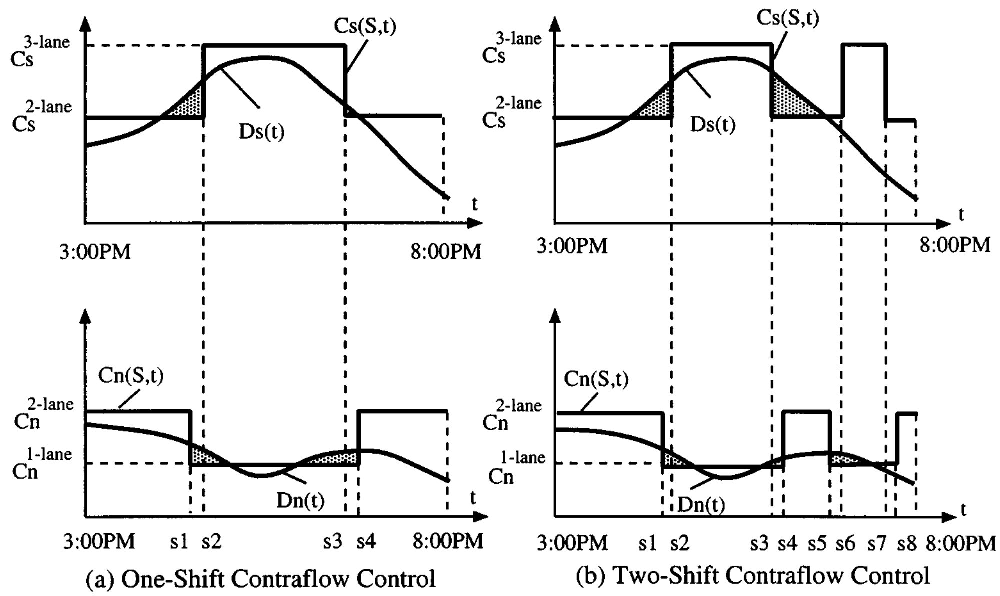

Fig. 6. Traffic demands and capacities at the tunnel site.

Steps 2)–4) are repeated continuously until the value of J_m reaches a minimum. The c final V_i vectors are then the patterns to be achieved.

C. Identification of the Optimal Pattern Number

An increase of the cluster number leads to a more accurate classification. However, a large number of clusters also needs more computation time during the identification of the best-fit pattern in real-time control. To balance these two contradict aspects, a method for identifying the optimal number of patterns is introduced.

The quality of a pattern clustering is evaluated using a newly introduced measure called *cluster concentration level* that represents the average distance of the data points to their pattern centers. Suppose the distance between a p-dimensional data point D_{ij} and its pattern center V_i is calculated by

$$\overline{d}_{ij} = \overline{d}(D_{ij}, V_i) = \sqrt{\frac{\sum_{k=1}^{p}(D_{ijk} - V_{ik})^2}{p}}. \tag{21}$$

The *cluster concentration level* $\overline{D}_c$ is defined as

$$\overline{D}_c = \frac{\sum_{i=1}^{c}\sum_{j=1}^{N_i}\overline{d}_{ij}}{N} \tag{22}$$

where

- N_i number of data points of the ith cluster;
- N number of all data points;
- c cluster number.

The cluster concentration level $\overline{D}_c$ decreases when the pattern number c increases. The relative decrease of the pattern concentration levels $\lambda(\overline{D}_c)$ is calculated by

$$\lambda(\overline{D}_c) = \frac{\overline{D}_{c-1} - \overline{D}_c}{\overline{D}_c}. \tag{23}$$

The optimal pattern number c^* is identified when $\lambda(\overline{D}_c)$ reaches its maximum.

D. Hierarchical Representation of Traffic Patterns

When the number of traffic patterns is large, it is inefficient to check all the patterns preserved at the same level for identifying the best-fit pattern. In this work, a hierarchical pattern representation method is introduced to improve pattern matching efficiency. In this method, all traffic data are first classified into a number of top-level patterns. If the number of data points in a pattern cluster is still large, a further classification is carried out, as illustrated in Fig. 5. Each pattern is described by its pattern center, V_i. The top level pattern clusters are linked together by a special root node.

The best matched pattern can be identified efficiently using a search through the illustrated clustering tree. Starting from the

TABLE I
TRAFFIC CONGESTION QUEUE LENGTH AT TIME t

Conditions	Queue Lengths $Q_i(\mathbf{S}, t)$
$D_i(t) - C_i(\mathbf{S}, t) \geq 0$	$Q_i(\mathbf{S}, t-1) + D_i(t) - C_i(\mathbf{S}, t)$
$D_i(t) - C_i(\mathbf{S}, t) < 0$ & $Q_i(\mathbf{S}, t-1) \leq C_i(\mathbf{S}, t) - D_i(t)$	0
$D_i(t) - C_i(\mathbf{S}, t) < 0$ & $Q_i(\mathbf{S}, t-1) > C_i(\mathbf{S}, t) - D_i(t)$	$Q_i(\mathbf{S}, t-1) - (C_i(\mathbf{S}, t) - D_i(t))$

(where i is either s or n for southbound or northbound direction.)

root node, the best matched subnode is identified using (14). The search process is carried out continuously until the best pattern at the bottom level is identified, as illustrated by the dark line in Fig. 5.

IV. Identification of the Optimal Contraflow Schedule Using Multilevel Constrained Optimization

The objective of contraflow control is to identify the optimal control parameters to minimize traffic delay at the traffic bottleneck. Different from a conventional optimization problem, both continuous and discrete variables are used in contraflow control, and the number of variables is also a variant.

A contraflow control schedule $\boldsymbol{S}$ is described by the number of contraflow shifts n and timing parameters in each shift. Since four steps are needed to complete a shift, the schedule of a shift is represented using four parameters $s_{i1}, s_{i2}, s_{i3}, s_{i4}$ $(i = 1, 2, \cdots, n)$.

Traffic delay at the bottleneck is calculated based on the difference between traffic demand and traffic capacity, as introduced in [7]. The traffic demands and capacities at the George Massey Tunnel in the afternoon, under one-shift and two-shift control schedules, are illustrated in Fig. 6. Since the traffic capacity at a certain time t is a function of the contraflow schedule $\boldsymbol{S}$, traffic delay at time t is also a function of the contraflow control schedule. Suppose $D_s(t)$ and $D_n(t)$ are traffic demands in southbound and northbound directions at time t, and $C_s(\boldsymbol{S}, t)$ and $C_n(\boldsymbol{S}, t)$ are the capacities in southbound and northbound directions at time t, the total traffic delay queue length $Q(\boldsymbol{S})$ during the time period $[T_1, T_2]$ can be calculated by

$$Q(\boldsymbol{S}) = \sum_{t=T_1}^{T_2} [Q_s(\boldsymbol{S}, t) + Q_n(\boldsymbol{S}, t)] \tag{24}$$

where $Q_s(\boldsymbol{S}, t)$ and $Q_n(\boldsymbol{S}, t)$ are the traffic delay queue length measures at time t in southbound and northbound directions, respectively. Their values are calculated using the equations given in Table I [7].

The optimization problem for a n-shift schedule $\boldsymbol{S_n}$ is thus formulated as

$$\min_{\text{w.r.t.}\boldsymbol{S_n}} Q(\boldsymbol{S_n}) = Q(s_{11}, s_{12}, \cdots, s_{n4})$$

subject to

$$\begin{aligned} &T_1 \leq s_{ij} \leq T_2 \qquad (i = 1, 2, \cdots, n;\ j = 1, 2, 3, 4) \\ &s_{i2} = s_{i1} + \Delta t \\ &s_{i3} = s_{i4} - \Delta t \end{aligned} \tag{25}$$

where Δt is the shift change-over time, a time between the close of a lane for clearing up traffic and the opening of this lane to traffic from the opposite direction. If the optimal schedule for a n-shift contraflow control is described as $\boldsymbol{S_n^*}$, the final optimal contraflow schedule, $\boldsymbol{S^*}$, considering all possible shift numbers is achieved by

$$Q(\boldsymbol{S^*}) = \min\{Q(\boldsymbol{S_1^*}), Q(\boldsymbol{S_2^*}), \cdots, Q(\boldsymbol{S_n^*})\}. \tag{26}$$

V. A Case Study: George Massey Tunnel Contraflow Control

A. Implementation of the George Massey Tunnel Contraflow Control System

The prototype George Massey Tunnel contraflow control system was developed based upon the introduced methods and implemented using C++ on a personal computer. The system and its user interface has been continuously improved by the BC Ministry of Transportation and Highways since then. On-line operation of the improved system at the George Massey Tunnel started in 1996 and achieved an excellent performance.

Traffic flow data are collected using 11 magnetic inductive loop traffic counters from the highway and the merging/exit roads near the tunnel. Each counter has six channels to record traffic flow data on different lanes. The 11 counters and their channels are labeled using counter numbers and channel index letters from A–F. The collected traffic data are sent to a central computer using modems and telephone lines.

The traffic network graphs for estimating current traffic demands are constructed based upon the layout of the road network. Fig. 7(a) shows the traffic network for southbound traffic demand estimation. These traffic counters are organized into three layers, for estimating southbound traffic demand using the equations given in Table II. The estimated traffic demands in the afternoon are shown in Fig. 2. Traffic demand estimation errors caused by congestion are eliminated by the multilayer dynamic traffic demand estimation model, where the threshold to detect the traffic congestion by comparing the traffic demands calculated with two neighboring layer traffic counters is set as 5%. Added or lost traffic is detected when the third layer counters are used. This error is compensated using a feedforward neural network, as shown in Fig. 7(b). In this research, 80 sampled data sets were used in training the neural network. The errors have been reduced from an average of 7% to less than 1%. The neural-network model was not implemented in the early version of the contraflow control system. Instead, the traffic loss compensation was carried out simply by multiplying a constant compensation factor, considering the relative traffic loss remains a constant.

The coming traffic demands at the tunnel site are achieved using the pattern matching method. Historical traffic flow data

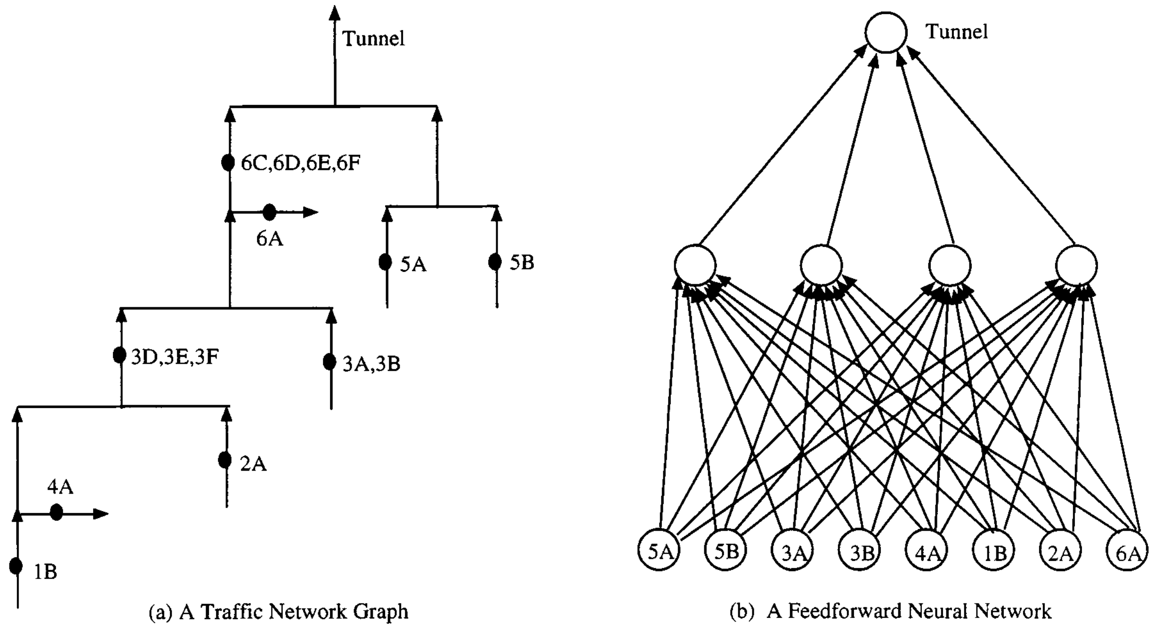

Fig. 7. Models for estimating traffic demand in southbound direction.

TABLE II
TRAFFIC DEMAND ESTIMATION MODELS USING THE THREE LAYER COUNTERS

Layers	Traffic demand Estimation Models
1	5A + 5B + 6C + 6D + 6E + 6F
2	5A + 5B + 3A + 3B + 3D + 3E + 3F − 6A
3	neural-net(5A, 5B, 3A, 3B, 2A, 1B, 4A, 6A)

are organized into two groups: 1) Mondays to Thursdays and 2) Fridays. These data are further clustered into nine and ten patterns, respectively. Each pattern is described by a vector with 85 elements, representing a sequence of vehicle counts from 4:00–11:00 a.m. and 1:00–8:00 p.m., respectively, with a 5-min interval.

The optimal contraflow schedule, consisting of the number of contraflow shifts and the timing parameters of each shift, is identified using the multilevel constrained optimization. Presently, only one-shift and two-shift control schedules are considered. The change-over time Δt is 10 min. The optimal contraflow control is activated between 5:30–10:30 a.m. and 3:00–8:00 p.m. The n-shift optimal contraflow control problem is solved using a derivative-based constrained optimization method considering computation efficiency for on-line operation and accuracy [15]. The system updates the on-line optimal schedule every 5 min through the active control period.

B. Evaluation of the George Massey Tunnel Contraflow Control System

The advantage of the proposed system can be illustrated by a comparison of the total traffic delay caused by three relevant contraflow control schemes, including: 1) the conventional fixed-time, one-shift contraflow control operation; 2) the presented real-time, optimal contraflow control method; and 3) the ideal optimal contraflow control schedule. Among these, the ideal optimal contraflow control schedule is obtained through an off-line contraflow control optimization using traffic data acquired directly from the tunnel site after the traffic has passed by. It has no engineering significance other than showing the potential of contraflow operation because it can only be carried out afterwards. The results of comparison is given in Table III. Although the presented real-time optimal contraflow control method can be further improved in principle, it does provide a significant improvement over the conventional fixed-time one-shift contraflow control method (around 34%).

TABLE III
TOTAL TRAFFIC DELAYS OF DIFFERENT CONTRAFLOW CONTROL SCHEMES

Conventional Fixed-Time, One-Shift Contraflow Control	2163
Presented Real-Time, Optimal Contraflow Control	1416
Ideal Optimal Schedule (in principle)	948
Improvement of the Proposed Method	34%
Room for Further Improvement (in principle)	22%

(Unit of Delay: Vehicle-hours)

VI. SUMMARY

A generic real-time optimal contraflow control method was introduced in this research to reduce congestion at traffic bottleneck sites. The current traffic demand at the bottleneck site is estimated using the nearby real-time traffic flow data collected by traffic counters. The demand estimation errors caused by congestion are compensated by a multilayer dynamic demand estimation model. The demand estimation errors caused by insufficient or malfunctioning traffic counters are compensated by a feedforward neural network. The coming traffic demand data are predicted by matching the collected traffic demand data with the traffic patterns that were achieved using fuzzy pattern clustering method. The optimal contraflow control schedule, including the shift number and timing parameters in each shift, is identified using a mixed-variable multilevel constrained optimization approach. The George Massey Tunnel contraflow control system, developed based upon the introduced method, has reduced the congestion considerably near the tunnel site.

ACKNOWLEDGMENT

The authors would like to thank Dr. W. W. Zhou, Highway Engineering Section Manager, and many others from the Ministry of Transportation and Highways of British Columbia, Canada for their contributions in specifying the George Massey Tunnel contraflow control problem and in implementing the prototype contraflow control system. These individuals include E. Miska, D. T. Yang, H. Zhang, J. Wu, Y. Cao, A. Lee, and L. Zhang.

REFERENCES

[1] OECD Scientific Expert Group, *Dynamic Traffic Management in Urban and Suburban Road Systems*. New York: OECD, 1987.
[2] Z. A. Sabra and C. R. Stockfisch, “Advanced traffic models: State-of-the-art,” *ITE J.*, pp. 31–42, Sept. 1995.
[3] P. T. Martin and S. L. M. Hockaday, “SCOOT—An update,” *ITE J.*, pp. 44–48, Jan. 1995.
[4] P. R. Lowrie, “The Sydney coordinated adaptive traffic system (SCATS)—Principles, methodology, and algorithms,” in *Proc. Int. Conf. Road Traffic Signaling*. London, U.K., 1982.
[5] “Intelligent Transportation Systems: Deployment and User Needs,” Transportation Res. Board, Nat. Res. Council, Washington, D.C., Transportation Res. Record 1537, 1996.
[6] D. J. Yang, “Dynamic measurements of the traffic demand through a highway bottle neck,” Tech. Rep., Ministry of Transportation and Highways of British Columbia, Victoria, Canada, Dec. 1992.
[7] W. W. Zhou, P. Livolsi, E. Miska, H. Zhang, J. Wu, and D. Yang, “An intelligent traffic responsive contraflow lane control system,” in *Proc. IEEE-Inst. Elect. Eng Vehicle Navigation Inform. Syst. Conf.*, Ottawa, Canada, 1993, pp. 174–181.
[8] Y. Cao, “Analysis of George Massey tunnel contraflow time changes,” Tech. Rep., Ministry of Transportation and Highways of British Columbia, Victoria, Canada, Aug. 1993.
[9] ——, “Estimating traffic demand off-line and on-line for George Massey tunnel,” Tech. Rep., Ministry of Transportation and Highways of British Columbia, Victoria, Canada, Sept. 1993.
[10] ——, “Real-time intelligent contraflow control of George Massey tunnel,” Tech. Rep., Ministry of Transportation and Highways of British Columbia, Victoria, Canada, Apr. 1994.
[11] ——, “Further report on real-time intelligent contraflow control of George Massey tunnel,” Tech. Rep., Ministry of Transportation and Highways of British Columbia, Victoria, Canada, Oct. 1994.
[12] D. Xue and Z. Dong, “Theoretical and implementational improvements to the George Massey tunnel contraflow system,” Tech. Rep., Department of Mechanical Engineering, University of Victoria and Ministry of Transportation and Highways of British Columbia, Victoria, Canada, Oct. 1994.
[13] P. K. Simpson, *Artificial Neural Systems*. Oxford, U.K.: Pergamon, 1990.
[14] J. C. Bezdek, *Pattern Recognition with Fuzzy Objective Function Algorithms*. New York: Plenum, 1981.
[15] J. S. Arora, *Introduction to Optimum Design*. New York: McGraw-Hill, 1989.